Simultaneous spectral analysis of multiple video sequence data for LWIR gas plumes

Sunu, Justin, Chang, Jen-Mei, Bertozzi, Andrea

Justin Sunu, Jen-Mei Chang, Andrea L. Bertozzi, "Simultaneous spectral analysis of multiple video sequence data for LWIR gas plumes," Proc. SPIE 9088, Algorithms and Technologies for Multispectral, Hyperspectral, and Ultraspectral Imagery XX, 90880T (13 June 2014); doi: 10.1117/12.2050149

SPIE.

Event: SPIE Defense + Security, 2014, Baltimore, Maryland, United States

Simultaneous spectral analysis of multiple video sequence data for LWIR gas plumes

Justin Sunu*, Jen-Mei Chang*, Andrea L. Bertozzi†,

ABSTRACT

We consider the challenge of detection of chemical plumes in hyperspectral image data. Segmentation of gas is difficult due to the diffusive nature of the cloud. The use of hyperspectral imagery provides non-visual data for this problem, allowing for the utilization of a richer array of sensing information. We consider several videos of different gases taken with the same background scene. We investigate a technique known as "manifold denoising" to delineate different features in the hyperspectral frames. With manifold denoising, we can bring more pertinent eigenvectors to the forefront. One can also simultaneously analyze frames from multiple videos using efficient algorithms for high dimensional data such as spectral clustering combined with linear algebra methods that leverage either subsampling or sparsity in the data. Analysis of multiple frames by the Nyström extension shows the ability to differentiate between different gasses while being able to group the similar items together, such as gasses or background signatures.

Keywords: Hyperspectral, data analysis, Nyström extension, manifold denoising, spectral clustering, image processing, video processing

1. INTRODUCTION

This work considers several data sets collected at the Dugway Proving Ground and provided to us by the Applied Physics Laboratory at Johns Hopkins University.[1] Video data was collected by long wave infrared spectrometers about two kilometers away from gas plume releases, at an elevation of about 1300 feet. The sensors capture one hyperspectral data cube every five seconds and the spectral measurements are taken in the long wave infrared portion of the spectrum, between 7830 nm and 11700 nm with a channel spacing of 30 nm. The spatial dimension of each data cube is 128×320 pixels with 129 spectral channels. It was demonstrated in a previous paper[2] that the clustering methods have the ability to isolate gas plumes within long wavelength hyperspectral video sequences. We also implemented a method to incorporate spatial information into the clustering methods, by means of feature vectors. Two issues arose from the work for which here we address. One is to improve spectral clustering results, especially in the case of diffuse gas plumes. The second is to incorporate temporal information, using information taken at other timesteps to get better clustering results. We implemented manifold denoising,[3] an inverse diffusion process designed to make a better separation of the eigenvectors of the graph Laplacian. In order to incorporate temporal information across multiple video frames, we developed a multiframe Nyström method[4] for computing eigenvectors of the graph Laplacian formed from all the pixels in these frames, thus connecting information across different timeframes. Several new and fast geometric algorithms have been proposed for data clustering,[5,6] building on spectral methods, and improved techniques for spectral clustering can be leveraged to yield better results in these classes of algorithms.[7]

Our experimental results are based upon three different releases shown in Figure 1. The aa gases were released with an explosion, whereas the sf6 was a gas release. The aa21 data set has a signature running through the middle of the frame that disrupts clusters from forming. In the case of Figure 1, the gas plume is split apart. The sf6 gas had a release that results in a very faint signature, making it difficult to differentiate from the background.

* Department of Mathematics and Statistics, California State University Long Beach, Long Beach, CA, USA
† Department of Mathematics, University of California Los Angeles, 520 Portola Plaza, Los Angeles, CA, USA

Algorithms and Technologies for Multispectral, Hyperspectral, and Ultraspectral Imagery XX, edited by Miguel Velez-Reyes, Fred A. Kruse, Proc. of SPIE Vol. 9088, 90880T · © 2014 SPIE · CCC code: 0277-786X/14/$18 · doi: 10.1117/12.2050149

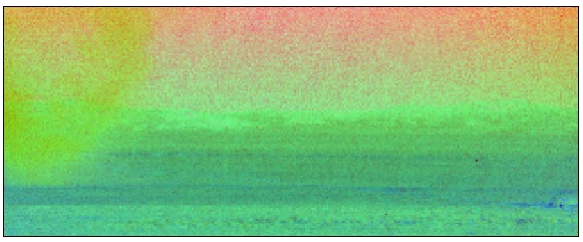

aa12 contains gas releases from an explosion

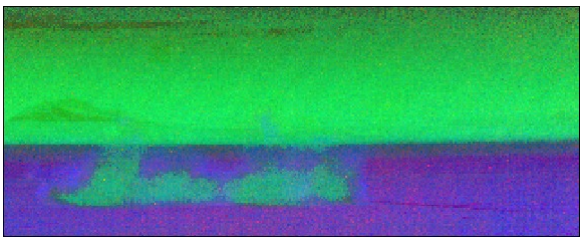

aa21 contains gas released from an explosion. Notice the disruptive portion

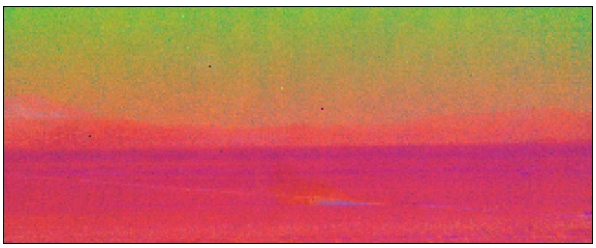

sf6-32 is a faint gas release

Figure 1: Types of gases released at the Dugway Proving Ground in Utah. The figure shown here are a false color visual representation of one video frame for each release.

2. BACKGROUND AND PREVIOUS WORK

In our previous work, we used K-means, spectral clustering, Nyström extension, and MBO on the Dugway Proving Ground data set. K-means was able to isolate the plume under ideal situations, but it had many problems and was unreliable. Spectral clustering[8,9] was able to provide good results, isolating the gas plume in many scenarios. The main issue for spectral clustering was when the plume became too diffuse and the outer edges of the gas plume were incorrectly clustered. The Nyström extension was much faster than spectral clustering, at the cost of accuracy within the results.

The main tool that we use here is the graph Laplacian computed from the hyperspectral pixel data. No spatial information is needed for the results here. We represent the data as nodes in a weighted graph, with each edge is assigned a measure of similarity $w(i,j)$ between each pair of vertices it is connecting. We use the Gaussian similarity formula

$$w(i,j) = e^{\frac{-|d_c(\mathbf{x},\mathbf{y})|^2}{2\sigma^2}}, \tag{1}$$

where the parameter $\sigma > 0$ is defined in the following sections. For this paper, the distance metric used is the cosine approximation, given by:

$$d_c(\mathbf{x},\mathbf{y}) = 1 - \frac{<\mathbf{x},\mathbf{y}>}{||\mathbf{x}||\ ||\mathbf{y}||}.$$

Where $\mathbf{x}$ and $\mathbf{y}$ define a pixel of the hyperspectral data. This approximation is faster to compute than the standard cosine distance, also known as the spectral angle. Because of the large volume of data and the size of the graph, it is important to implement a formula that reduces compute time.

3. MANIFOLD DENOISING ALGORITHM

3.1 Motivation

The graph Laplacian is very important when it comes to graph based algorithms, it is the starting point for some of these algorithms. One example of a denoising method that directly uses the graph Laplacian is manifold denoising.[3] Here we find that this method provides reasonable separation of features in each frame of the video sequence while offering an added benefit. A problem in clustering the gas plume is when the plume becomes diffuse. The gas signature is not strong enough to be categorized as gas, therefore it needs to be strengthened or enhanced. After this enhancement, the border of the gas plume should be well defined and gas cluster should be filled in, without holes. Manifold denoising accomplishes this.

3.2 Algorithm

This method works by performing a forward diffusion process. The algorithm for manifold denoising is described in Algorithm 1. The idea for this method is to use the graph Laplacian in place of the Laplace operator, Δ, in the heat equation, and solve the system of equations for the previous timestep. We consider the heat equation applied to the old time level in which the Laplace operator is computed from the old data:

$$\frac{\partial u}{\partial t} + a\Delta_n u = 0.$$

We solve this using a semi-implicit timestep according to the scheme:

$$\frac{u(t+1) - u(t)}{\delta t} = -a\Delta_n u(t+1).$$

Some algebraic manipulations lead to the simple expression:

$$(1 + \delta t\Delta_n)^{-1} D_n = D_{n+1}.$$

Where D_n represents the current iteration of the data set, D_{n+1} represents the next iteration of the data set, and Δ_n represents the current graph Laplacian. Due to the size of the graph Laplacian, it is not computationally feasible to obtain the inverse directly. As an alternative, we solve D_{n+1} in MATLAB with its built-in method for solving a sparse system of equations followed by a factorization with backward-forward substitution.

Algorithm 1 Manifold denoising algorithm[3]

Data set $D = D_0$, stopping criterion ϵ, constant δt
while Stopping criterion not satisfied **do**
  Compute the graph Laplacian, Δ
  Solve the system of linear equations

$$D_{n+1} = (\mathrm{I} + \delta t\Delta)^{-1} D_n$$

  Check the stopping criterion,

$$\max(D_{n+1} - D_n) < \epsilon$$

end while

3.3 Results

The goal for manifold denoising is to achieve a better separation between the background and gas plume. After experimentation, there were two additional benefits to using this approach. One is the ability to form graph connections, for example a with strong interference causes the gas plume to be broken in two separate clusters. After applying manifold denoising, there were enough overlapping clusters to potentially join the two into one cluster. The second benefit was bringing forth important eigenvectors. In another sample frame, the gas plume eigenvector was uncovered by the 26th eigenvector. After applying manifold denoising, the gas plume eigenvector was located in the fourth location, a much more prominent position. Our modified spectral clustering algorithm only uses the k nearest neighbors instead of the full graph Laplacian. Because of this, the parameter, σ, can be chosen with much flexibility. The values we found that worked well were between 0.01 and 100.

Figure 2 shows the progressions of manifold denoising applied to the specific plume eigenvector. The final result captures the plume in its entirety, even in the areas where the signature is too diffuse to properly make the distinction. Figure 3 shows the results on the sf6 data. The first six iterations show what the gas plume is presumed to be, within the first 25 eigenvectors of the graph Laplacian. After 6 iterations, the actual gas plume enters the top 25 eigenvectors, and after the 10th iterations, allows for a clear separation of the gas plume and background. Figure 4 shows the spectral clustering method applied to the aa21 data set, without denoising. One difficulty is the lack of connections being made between the top and bottom half of the gas plume. Attempts with K-means to consolidate these connections still result in the top and bottom of the gas plume to show up in different clusters. Figure 5 shows the results after manifold denoising. After applying K-means onto these results, we obtained the clustering shown in Figure 6. These results show that there are connections being made between the top and bottom half of the plume, despite the strong change in signal across the middle of the frame.

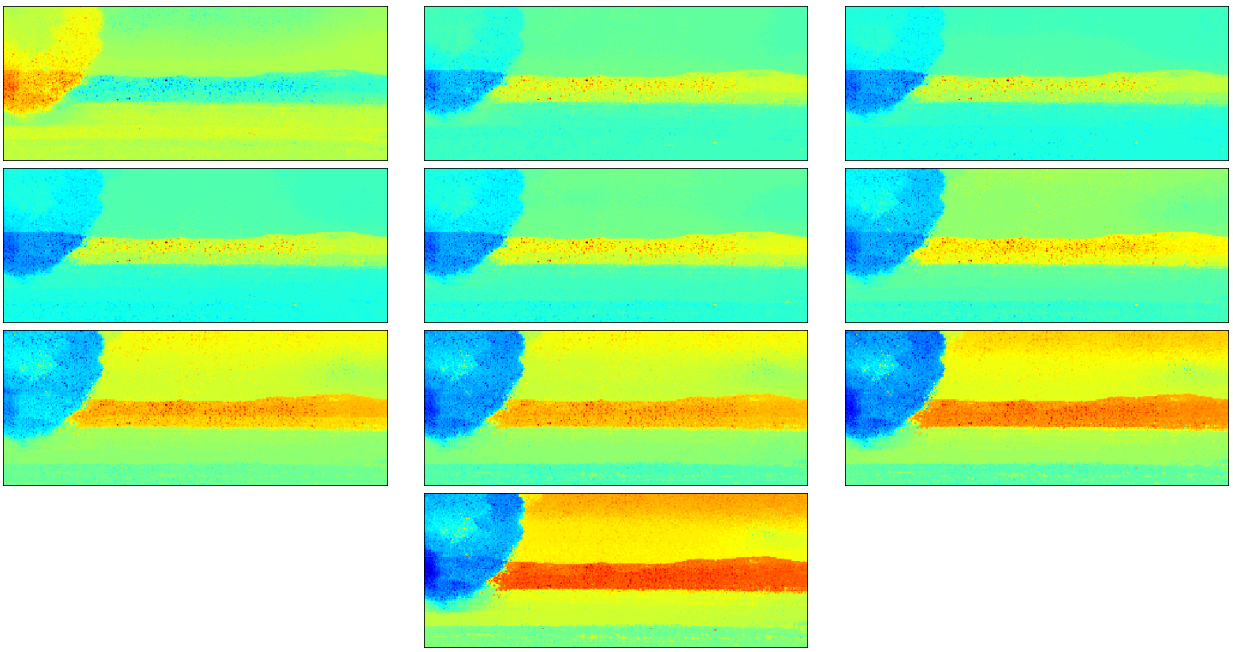

Figure 2: The spectral clustering result after iterations of manifold denoising on aa12. Shown are the gas plume eigenvectors.

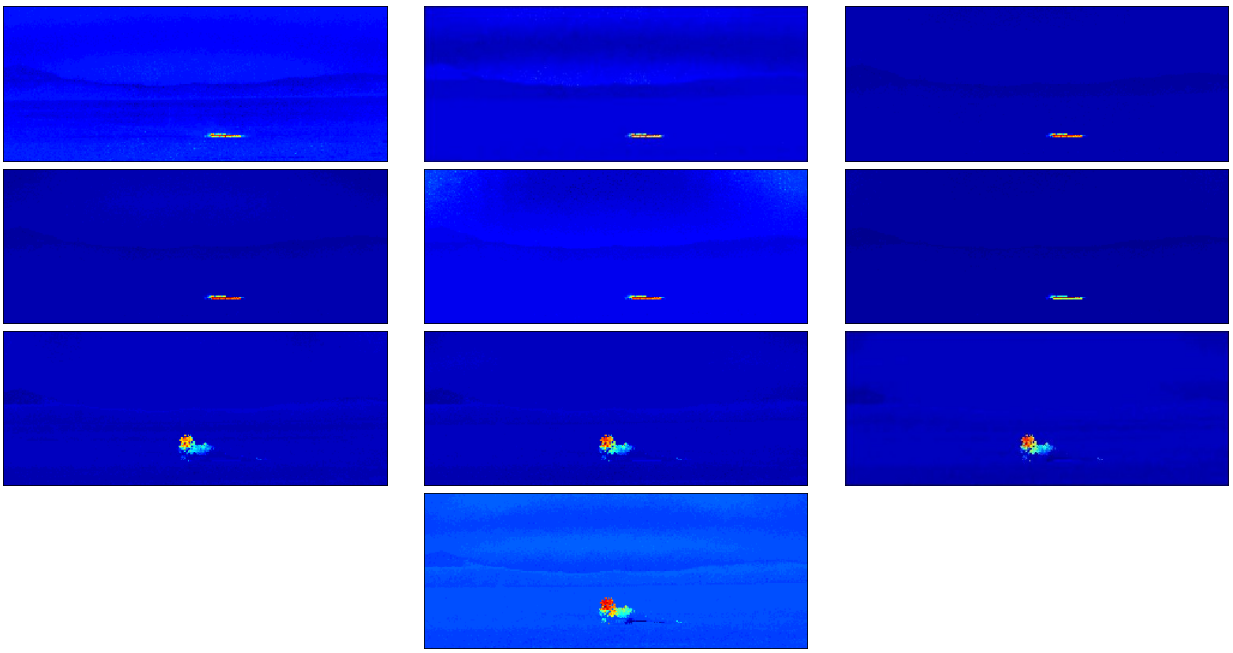

Figure 3: Results of Spectral Clustering with Manifold Denoising on sf6-32. Shown are the supposed gas plume eigenvectors.

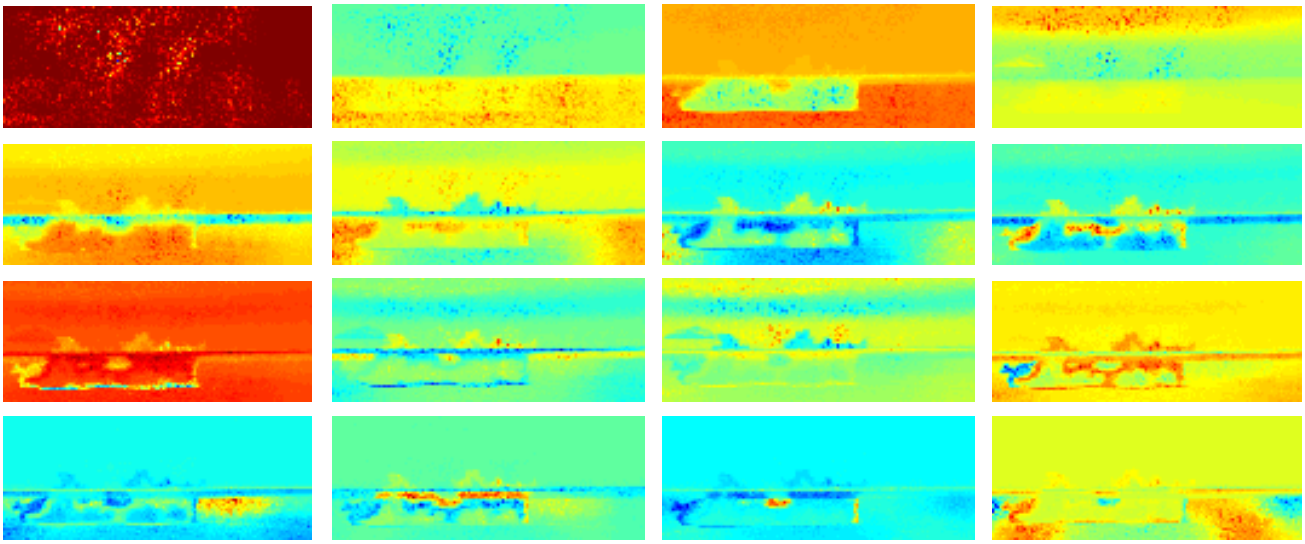

Figure 4: Spectral clustering results on the aa21 data set, first 16 eigenvectors.

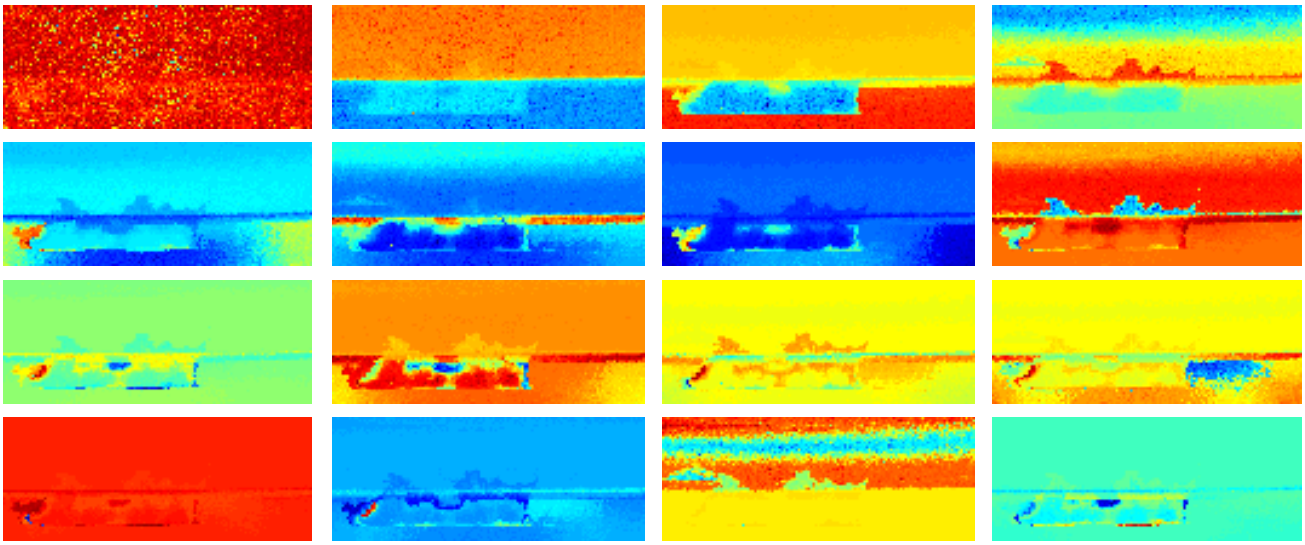

Figure 5: Spectral clustering results after manifold denoising on the aa21 data set, first 16 eigenvectors.

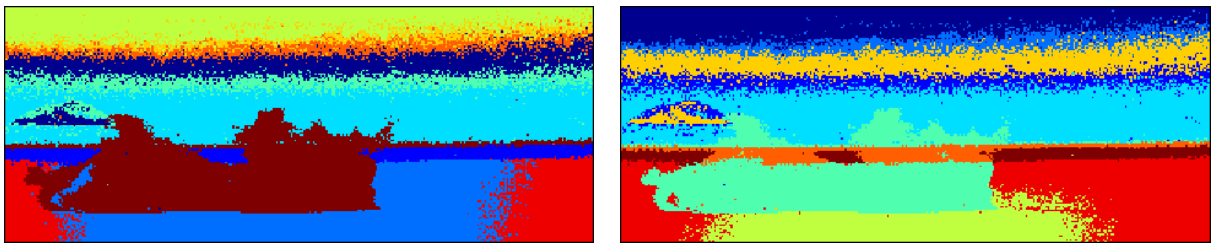

Figure 6: Sample K-means on the eigenvectors of the graph Laplacian of aa21 after denoising.

4. MULTIFRAME NYSTRÖM

4.1 Motivation

In our previous work[2] we implemented feature vectors in order to incorporate spatial information. Now the goal is to use temporal information, by means of multiframe clustering. Since this is hyperspectral data, temporal information can be limited in use, since it depends heavily on temperature at the time of day. Thus we look at a series of seven frames rather than the entire video data set.

4.2 Algorithm

The algorithm for multiframe analysis is explained in Algorithm 2, and the algorithm for Nyström extension is explained Algorithm 3. The idea for multiframe analysis is to form a large matrix with multiple frames from the video sequence, to incorporate information of the data at different times. However, the large size of the concatenated matrix makes it impossible to directly perform spectral clustering (on the full similarity matrix) with modest desktop processors, thus the Nyström extension is used. The Nyström extension computes an approximation for the eigenpairs of the graph Laplacian. In other words, it forms an approximate spectral clustering results. The Nyström extension works by selecting a small random sample and using this sample to perform a method of matrix completion for the graph Laplacian. Afterwards it approximates the eigenpairs for this approximed graph Laplacian. The Nyström extension is many times faster than spectral clustering, and uses less memory, allowing for large scale spectral analysis to be performed.

Algorithm 2 Multiframe analysis

Select $K-1$ consecutive frames from a video sequences, and 1 background frame
Reformat the hypercubes into a row of matrices
Concatenate all of the row matrices into one large matrix, M
Perform clustering on the newly formed matrix, M

Algorithm 3 Nyström extension[4]

Randomly select k data points to form the set A, while the rest of data forms the set B
Compute distances amongst data in A, named D_A and distances between data in A and B, named D_B
Approximate the distances amongst data in B, D_C, with $D_C = D_B^T D_A^{-1} D_B$
Compute the row sum of the matrix L, where $d_i = \sum_{j=1}^{n} L_{i,j}$
Normalize the elements of D_A and D_B, named $\overline{D_A}$ and $\overline{D_B}$, respectively
Setting $Q = \overline{D_A} + \overline{D_A}^{-.5} * \overline{D_B} * \overline{D_B}^T * \overline{D_A}^{-.5}$, find the singular value decomposition, $Q = USV^T$
Compute $V = \begin{bmatrix} \overline{D_A} \\ \overline{D_B}^T \end{bmatrix} \overline{D_A}^{-.5} U L^{-.5}$
Compute the eigenvector approximation $Eig = \frac{V_i}{V_{1i}(1-L_{ii})^{.5}}$

4.3 Results

Figure 7 shows the results of multiframe Nyström being applied to seven hyperspectral video frames. The seven frames are composed of six sequential gas plume frames as well as one background frame taken before the gas plume is released. Each column represents one eigenvector, reshaped for easier viewing of the results. The best σ parameter was found to be $\sigma = .01$. These results show that Nyström was able to group like objects together across the different frames, even showing the lack of gas plume in the first frame. One of the greatest difficulties working with the eigenvectors of the graph Laplacian is that there is no continuity from one frame to the next, the second eigenvector in one frame can be the fourth in another. This makes for analysis across frames very challenging; multiframe Nyström removes this problem.

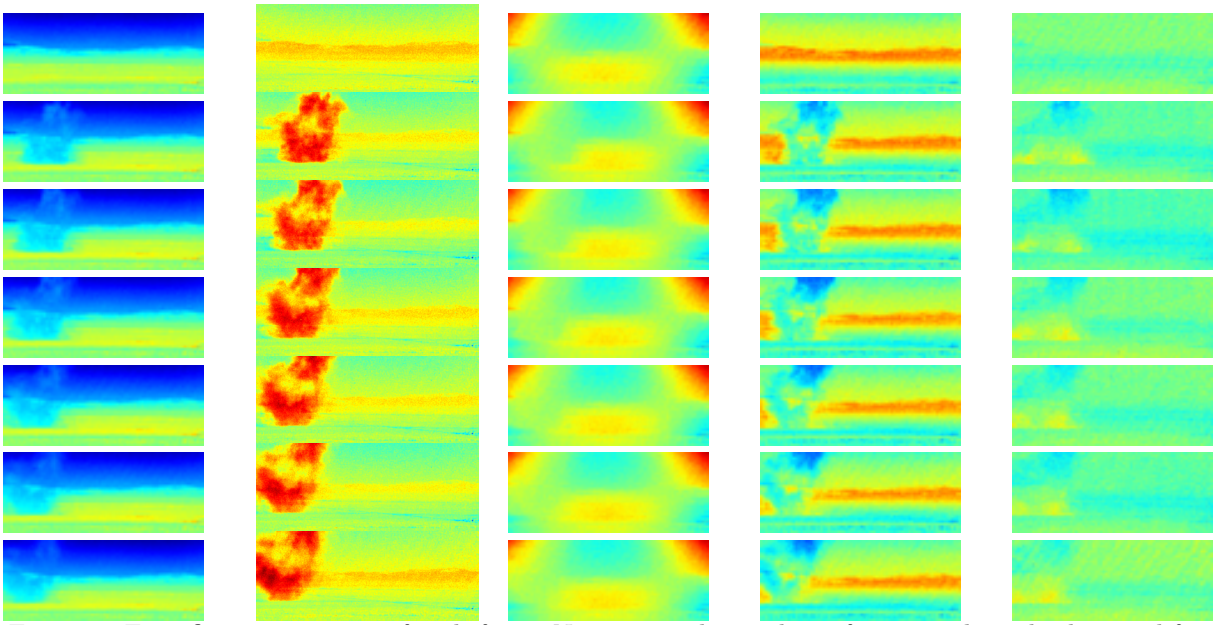

Figure 7: First five eigenvectors of multiframe Nyström with six plume frames and one background frame.

5. CONCLUSION AND FUTURE WORK

Manifold denoising is an iterative method that is able to improve the quality of spectral algorithms applied to hyperspectral data. It allows for better delineation in clustering results, improving the ordering of graph Laplacian eigenvectors, and making connections between broken segments. The multiframe Nyström provides a nice continuous segmentation across different frames, allowing for the incorporation of temporal information. One can use these results in more complex methods that are built on spectral information. An example of this is the implementation of multiclass MBO to the multiframe results.[7] For future work, a challenge in using the manifold denoising method is the choice of stopping criterion for the iteration. At this point, the max of the differences does not always provide a good place to stop. In this work we sometimes used a human in the loop to define the best number of iterations. Another interesting line of inquiry is to incorporate spatial information (feature vectors) along with the multiframe components, allowing for both temporal and spatial information to be grouped together. The visual results we generated with the multiframe Nystrom method provided unprecedented insights into the nature of the data set. This is especially valuable particularly because the method assumes no prior knowledge on the gas signatures.

6. ACKNOWLEDGEMENTS

This project was funded by NSF grants DMS-0914856, DMS-1118971, and DMS-1045536, Office of Naval Research (ONR) grants N000141210040 and N000141210838, and UC Lab Fees Research grant 12-LR-236660.

REFERENCES

[1] J. B. Broadwater, D. Limsui, and A. K. Carr., *A primer for chemical plume detection using LWIR sensors*, Technical report, National Security Technology Department, 2011.

[2] T. Gerhart, J. Sunu, L. Lieu, E. Merkurjev, J.-M. Chang, J. Gilles, A. L. Bertozzi, *Detection and tracking of gas plumes in LWIR hyperspectral video sequence data*, SPIE Conference on Defense Security and Sensing, 2013, Baltmore, MD, April 29-May 3, 2013.

[3] M. Hein and M. Maier,*Manifold denoising*, In Advances in Neural Information Processing Systems (NIPS) 19. MIT Press. 5, 2006.

[4] C. Fowlkes, S. Belongie, F. Chung, and J. Malik., *Spectral grouping using the Nyström method.*, IEEE Trans. Pattern Analysis and Machine Intelligence, Vol. 26, No. 2 (2004): 214-225.

[5] C. Garcia-Cardona, E. Merkurjev, A. L. Bertozzi, A. Flenner and A. G. Percus, *Multiclass Data Segmentation Using Diffuse Interface Methods on Graphs*, IEEE Trans. Pattern Anal. Mach. Int., 2014.

[6] E. Merkurjev, C. Garcia, A. L. Bertozzi, A. Flenner, A. Percus, *Diffuse interface methods for multiclass segmentation of high-dimensional data*, Applied Math. Letters, online first, March 4, 2014.

[7] E. Murkerjev, J. Sunu, and A.L. Bertozzi, *Graph MBO method for multiclass segmentation of hyperspectral stand-off detection video*, preprint, 2014.

[8] Ulrike von Luxburg, *A tutorial on spectral clustering.*, Statistics and computing 17, no. 4 (2007): 395-416.

[9] A. Y. Ng, M. I. Jordan, and Y. Weiss., *On spectral clustering: Analysis and an algorithm.*, Advances in neural information processing systems 2 (2002): 849-856.